arXiv:astro-ph/0312136v2 6 Dec 2003

The central image of a gravitationally lensed quasar

Joshua N. Winn[1], David Rusin[1,2], Christopher S. Kochanek[1,3]

[1]Harvard-Smithsonian Center for Astrophysics, Cambridge, MA 02138, USA
[2]Dept. of Physics and Astronomy, University of Pennsylvania, Philadelphia, PA 19104, USA
[3]Dept. of Astronomy, The Ohio State University, Columbus, OH 43210, USA

A galaxy can act as a gravitational lens, producing multiple images of a background object. Theory predicts there should be an odd number of images[1,2] but, paradoxically, almost all observed lenses have 2 or 4 images. The missing image should be faint and appear near the galaxy's center. These "central images" have long been sought as probes of galactic cores too distant to resolve with ordinary observations.[3,4,5,6,7] There are five candidates, but in one case the third image is not necessarily a central image,[8,9,10] and in the others, the central component might be a foreground source rather than a lensed image.[11,12,13,14,15] Here we report the most secure identification of a central image, based on radio observations of PMN J1632–0033, one of the latter candidates. Lens models incorporating the central image show that the mass of the lens galaxy's central black hole is $<2\times10^8$ solar masses ($M_\odot$), and the galaxy's surface density at the location of the central image is $>20{,}000 M_\odot$ per square parsec, in agreement with expectations based on observations of galaxies hundreds of times closer to the Earth.

Central images are often called "odd" images, but the key property that makes them interesting is not their odd number, but rather their proximity to the center of the lens galaxy. To emphasize the distinction, we note that there can be an odd number of images without any central images, if the gravitational field has a large quadrupole[9] or if there are multiple lens galaxies[16,17].

The absence of central images is a problem dating to the earliest days of galaxy lens observations, and many solutions have been proposed.[3,18,19] Most recently, Evans & Hunter[6] and Keeton[7] argued that the absence of central images at current detection limits is no longer surprising, given recent *Hubble Space Telescope* observations of nearby galaxies.[20] Those observations showed that the distribution of stars near the centers of massive elliptical galaxies (the predominant type of lens galaxy) is highly concentrated. Because the central image flux depends inversely on the square of the surface density, the concentrated density profiles should cause central images to be very faint (or even to have zero flux, if the density is singular), and detection limits will need to be improved by a factor of 10–50 before central images are commonly seen. In the meantime, the most favorable systems are radio-loud double quasars with large flux ratios. Radio waves are not extinguished by dust or overpowered by light in the lens galaxy, and asymmetric doubles produce the brightest possible central image for a given mass distribution.

One such system is PMN J1632–0033.[14] It has two images (A and B) of a radio-loud quasar at redshift 3.42, with a flux ratio of 13. The lens redshift is unknown; our working assumption is $z_L = 1.0$, as estimated by requiring the galaxy's photometry and mass to be consistent with the fundamental plane of elliptical galaxies.[14] There is also a faint radio component (C) with a position and flux appropriate for a central image. However, as in a few other systems,[11,12,13] the possibility could not be excluded that C is an active galactic nucleus (AGN) in the lens galaxy rather than a third quasar image.[15] The simplest test is to compare the continuum radio spectra of the components. Because lensing preserves the frequency of photons, lensed images have the same spectrum (in the absence of differential propagation effects) whereas there is no reason why a foreground AGN would have the same spectrum as a background source.

Previously we attempted this comparison at frequencies from 1.7 to 15 GHz, finding that C was fainter at low frequency than expected for a third image.[15] However, the discrepancy was limited to a single measurement at the lowest frequency, where radio propagation effects are strongest. A central image might be affected more than other images by scintillation or absorption, due to its passage through the dense galactic center. Thus we could make no firm conclusion before obtaining data at higher frequencies, where propagation effects (scaling characteristically as ν^{-2}) are negligible.

We have now extended our measurements to 22 and 43 GHz, and obtained additional data at 8 and 15 GHz, using the Very Large Array (VLA). The high-frequency spectrum of the central component agrees well with those of the bright quasar images. For $\nu > 1.7$ GHz, the logarithmic slopes of flux density ratio *vs.* frequency (which should be zero for lensed images) are 0.00 ± 0.04 for B/A and -0.02 ± 0.07 for C/A. This is powerful evidence that C is a third quasar image.

The evidence that C is not only a *third* image, but also a long-sought *central* image, is its proximity to the center of the lens galaxy ($\lesssim$30 milli-arcseconds), and its faintness (0.41% the flux density of A). This sets PMN J1632–0033 apart from the only other three-image system known, APM 08279+5255, in which the lens galaxy has not been detected, and the fluxes of all three images are of the same order of magnitude. This leaves open the possibility that the third image in that system is not a central image, but rather a "naked-cusp" image due to a highly flattened mass distribution.[8,9]

For PMN J1632–0033, the central image properties can be used to constrain the core structure of the lens galaxy. In general this requires detailed modeling, for which we refer the reader to Ref. 15, in which some consequences of the central-image hypothesis were worked out before the status of C was clarified. Here we quote one result, and elaborate upon it to include the effect of a central black hole. If the mass distribution is taken to be a spherical power law, $\rho(r) \propto r^{-\beta}$, embedded in an external shear field to account for non-sphericity, then the data require $\beta = 1.91 \pm 0.02$ (2σ confidence), only slightly shallower than an isothermal ($\beta = 2$) mass distribution. The uncertainty is far smaller for this system than for typical two-image or four-image systems, because of the sensitive dependence of the central-image magnification on the exponent of the central cusp.

If the central mass were too large, then either a bright fourth image would be produced, or the central image would be de-magnified out of existence.[3,6,7,21] This fact can be used to derive an upper limit on the mass of any central black hole. We added a central point mass to the power-law model described above, finding that the limits on β are barely affected and $M_{\rm BH} < 2.0 \times 10^8 M_\odot$.

How does this compare to the mass of the black hole that is expected to reside in this galaxy? Among nearby galaxies, $M_{\rm BH}$ is correlated with the velocity dispersion of the surrounding stellar bulge.[22,23] The exact correlation is a matter of debate, but for present purposes we adopt the correlation of Tremaine *et al.*[24] Since the mass distribution of the lens galaxy in PMN J1632–0033 appears to be nearly isothermal, the A–B angular separation $\Delta\theta = 1.46$ arc seconds can be used to estimate σ via the relation $\Delta\theta/2 = (4\pi\sigma^2/c^2)(D_{\rm LS}/D_{\rm S})$, where $D_{\rm LS}$ and $D_{\rm S}$

are the lens–source and observer–source angular diameter distances. Assuming a flat $\Omega_{\rm M} = 0.3$ cosmology with $H_0 = 72$ km s^{-1} Mpc^{-1} and $z_{\rm L} = 1.0$, the results are $\sigma = 224$ km s^{-1} and $M_{\rm BH} = (2.1 \pm 0.4) \times 10^8 M_\odot$. Thus, the black hole cannot be much larger than expected from the local correlation.

A simple argument can also be used to place a *lower* bound on the core density of the galaxy. Since the density presumably does not increase with radius, the minimum central density occurs for the case of a constant-density core, for which the magnification of C is $\mu_{\rm C} = (1-\kappa_{\rm C})^{-2}$. Here, κ is the surface density, in units of the cosmology- and redshift-dependent critical surface density for lensing. The near-isothermal models give $\mu_{\rm C} = 0.0082$, from which it follows $\kappa_{\rm C} > 10$. Under the same cosmological assumptions as above, the surface density is $>$20,000 $M_\odot$ pc^{-2} within the radius of C. The radius of C is not known accurately but is $\lesssim$30 mas, corresponding to $\lesssim$230 pc, or $\lesssim 0.15 R_{\rm eff}$, where $R_{\rm eff}$ is the effective radius of the galaxy.

How does this compare to nearby galaxy cores observed with *HST*? Among the sample of Faber *et al.*[20] are 38 early-type (E/S0) galaxies with measurements of core surface brightness profile, $R_{\rm eff}$, and velocity dispersion. We used their estimates of the mass-to-light ratio (derived from the velocity dispersion) to convert the surface brightness profile into a surface density profile. At $R/R_{\rm eff} = 0.15$, the surface densities range from 10^3 to 10^5 $M_\odot$ pc^{-2}, showing that our result is consistent with local estimates and astrophysically relevant.

Thus we have derived limits on surface density and black-hole mass of the lens galaxy (comoving distance $\sim$3 gigaparsecs) that are consistent with more detailed measurements possible only for nearby galaxies ($\sim$30 megaparsecs). The lensing constraints have the advantage of depending directly on mass, rather than light. This motivates the discovery of additional central-image systems, and further observations of this system, some of which we describe below.

The most immediate challenges are direct measurement of the lens redshift and more accurate ($\lesssim$5 mas) measurement of the position of C relative to the lens center. These data would better pin down the physical radius within which the limits on surface density apply, and firm up the correspondence with nearby galaxies.

Measuring correlated variability between C and another image would provide irrefutable evidence that C is a central image, should doubt still remain. Because of the different light-travel times, quasar flux variations should be seen first in A, then $\approx$180 days later in B, and then $\approx$9 hours later in C. The ratio of the delays would also further constrain mass models, although the C–B delay measurement would be difficult due to the faintness of the image and the necessarily fine time-sampling.

Finally, an additional image[21] is predicted to occur over the entire allowed range of parameters of our models with central black holes. In general, the fourth image has $<$10% the flux of C, although there are very rare arrangements in which C represents a pair of merging images. It is separated by $<$20 mas from C, indicating the need for very-long-baseline interferometry. Currently, the strongest upper limit on the flux of an additional component is $<$30% that of C, based on the 5σ limit at 8 GHz.[15] Detection of the fourth image would be interesting because the separation and magnification ratio between the central images would provide a measurement of $M_{\rm BH}$, rather than an upper limit.

Received 26 September 2003; Accepted 2 December 2003.

1. Dyer, C.C. & Roeder, R.C. Possible multiple imaging by spherical galaxies. *Astroph. J.*, **238**, L67–L70 (1980).
2. Burke, W.L. Multiple gravitational imaging by distributed masses. *Astroph. J.*, **244**, L1 (1981).
3. Narasimha, D., Subramanian, K., & Chitre, S.M. “Missing image” in gravitational lens systems? *Nature*, **321**, 45–46 (1986).
4. Wallington, S. & Narayan, R. The influence of

core radius on gravitational lensing by elliptical lenses. *Astroph. J.*, **403**, 517–529 (1993).

5. Rusin, D. & Ma, C.-P. Constraints on the inner mass profiles of lensing galaxies from missing odd images. *Astroph. J.*, **549**, L33–L37 (2001).
6. Evans, N.W. & Hunter, C. Lensing properties of cored galaxy models. *Astroph. J.*, **575**, 68–86 (2002).
7. Keeton, C.R. Lensing and the centers of distant early-type galaxies. *Astroph. J.*, **582**, 17–29 (2003).
8. Muñoz, J.A., Kochanek, C.S., & Keeton, C.R. Cusped mass models of gravitational lenses. *Astroph. J.*, **558**, 657–665 (2001).
9. Lewis, G.F., Carilli, C., Papadopoulos, P., & Ivison, R.J. Resolved nuclear CO(1–0) emission in APM 08279+5255: gravitational lensing by a naked cusp? *Mon. Not. R. Astr. Soc.*, **330**, L15–L18 (2002).
10. Lewis, G.F., et al. Spatially resolved STIS spectra of the gravitationally lensed broad absorption line quasar APM08279+5255: the nature of component C and evidence for microlensing. *Mon. Not. R. Astr. Soc.*, **334**, L7–L10 (2002).
11. Gorenstein, M.V., et al. Detection of a compact radio source near the center of a gravitational lens: quasar image or galactic core? *Science*, **219**, 54–56 (1983).
12. Chen. G. & Hewitt, J.N. Multifrequency radio images of the Einstein ring gravitational lens MG 1131+0456. *Astroph. J.*, **106**, 1719–1728 (1993).
13. Fassnacht, C., et al. B2045+265: A New Four-Image Gravitational Lens from CLASS. *Astron. J.*, **117**, 658–670 (1999).
14. Winn, J.N., et al. PMN J1632–0033: a new gravitationally lensed quasar. *Astron. J.*, **123**, 10–19 (2002).
15. Winn, J.N., Rusin, D., & Kochanek, C.S. Investigation of the possible third image and mass models of the gravitational lens PMN J1632-0033. *Astroph. J.*, **587**, 80–89 (2003).
16. Winn, J.N., Kochanek, C.S., Keeton, C.R., & Lovell, J.E.J. The quintuple quasar: radio and optical observations. *Astroph. J.*, **590**, 26–38 (2003).
17. Keeton, C.R. & Winn, J.N. The quintuple quasar: mass modeling and interpretation. *Astroph. J.*, **590**, 39–51 (2003).
18. Narayan, R., Blandford, R., & Nityananda, R. Multiple imaging of quasars by galaxies and clusters. *Nature*, **310**, 112–115 (1984).
19. Subramanian, K., Chitre, S.M., & Narasimha, D. Minilensing of multiply imaged quasars: flux variations and vanishing of images. *Astroph. J.*, **289**, 37–51 (1985).
20. Faber, S., *et al.* The centers of early-type galaxies with HST. IV. Central parameter relations. *Astron. J.*, **114**, 1771–1796 (1997).
21. Mao, S., Witt, H.J., & Koopmans, L.V.E. The influence of central black holes on gravitational lenses. *Mon. Not. R. Astr. Soc.*, **323**, 301–307.
22. Ferrarese, L. & Merritt, D. A fundamental relation between supermassive black holes and their host galaxies. *Astroph. J.*, **539**, L9–L12 (2000).
23. Gebhardt, K., et al. A relationship between nuclear black hole mass and galaxy velocity dispersion. *Astroph. J.*, **539**, L13–16 (2000).
24. Tremaine, S., et al. The slope of the black hole mass versus velocity dispersion correlation. *Astroph. J.*, **574**, 740–753 (2002).
25. Mezger, P.G. & Henderson, A.P. Galactic H II regions. I. Observations of their continuum radiation at the frequency 5 GHz. *Astroph. J.*, **147**, 471–489.
26. Beckert, T. et al. Anatomy of the Sagittarius A complex. V. Interpretation of the Sgr A* spectrum. *Astron. & Astroph.*, **307**, 450–458.
27. Taylor, G.B. The symmetric parsec-scale jets of the radio galaxy Hydra A. *Astroph. J.*, **470**, 394–402.
28. Walker, R.C. et al. VLBA absorption imaging of ionized gas associated with the accretion disk in NGC 1275. *Astroph. J.*, **530**, 233–244.

Acknowledgements

The authors are grateful to S. Doeleman and P. Schechter for helpful discussions, and J. Bullock for comments on the manuscript. J.N.W. acknowledges the support of the National Science Foundation (NSF) through an Astronomy & Astrophysics Postdoctoral Fellowship. The VLA is part of the National Radio Astronomy Observatory, an NSF facility operated under cooperative agreement by Associated Universities, Inc.

Correspondence should be addressed to J.N.W. (e-mail: jwinn@cfa.harvard.edu).

Date (UT)	Frequency (GHz)	A (mJy)	B (mJy)	C (mJy)	R.M.S. noise (mJy beam^{-1})
2003 Jul 23	8.46	202.13	16.49	0.84	0.033
2003 Aug 02	8.46	209.82	16.65	0.74	0.040
2003 Aug 30	8.46	195.19	15.86	0.78	0.042
2003 Jun 10	14.94	173.27	12.50	0.72	0.16
2003 Jul 01	14.94	180.17	13.87	0.57	0.13
2003 Jun 12	22.46	149.54	10.78	0.62	0.076
2003 Jun 24	22.46	146.95	10.81	0.48	0.061
2003 Jun 26	22.46	146.42	10.78	0.66	0.066
2003 Jun 15	43.34	107.25	7.85	0.38	0.077

Table 1. Radio observations of PMN J1632–0033 with the Very Large Array. The array was in the A configuration. The primary flux density calibrator was 3C 286 and the phase calibrator was J1658+0741 (except the 8 GHz observation of 2003 Jul 23, for which it was J1651+0129). Initial calibration was performed with standard AIPS procedures. Further self-calibration and imaging were performed with Difmap. Flux densities were determined by fitting a model consisting of 3 point sources to the visibility data. For the 8 GHz and 15 GHz data, the relative positions of the components were fixed at the values determined by previous higher resolution measurements[14].

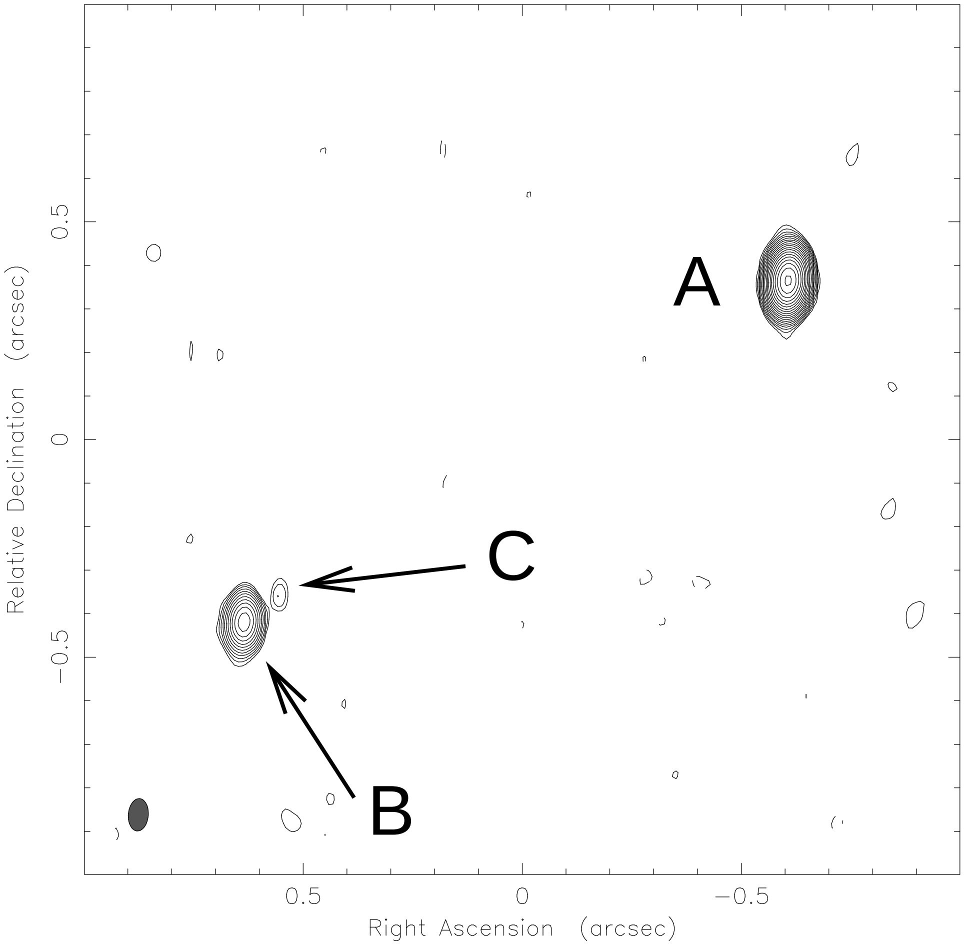

Figure 1. A radio map of the three components of gravitational lens PMN J1632–0033. The observations were carried out with the VLA at 43 GHz, with a total bandwidth of 100 MHz. Standard phase and amplitude calibration were applied, and the map was created with natural weighting. The root-mean-squared (RMS) noise level in the residual map is $\sigma = 0.077$ mJy beam^{-1}, as compared to the theoretical minimum RMS of 0.04 mJy beam^{-1}. Contour levels begin at 2.5σ and increase by powers of $\sqrt{2}$. The synthesized beam (full width at half-maximum of 0.073×0.044 arc seconds) is illustrated in the lower left corner of the map.

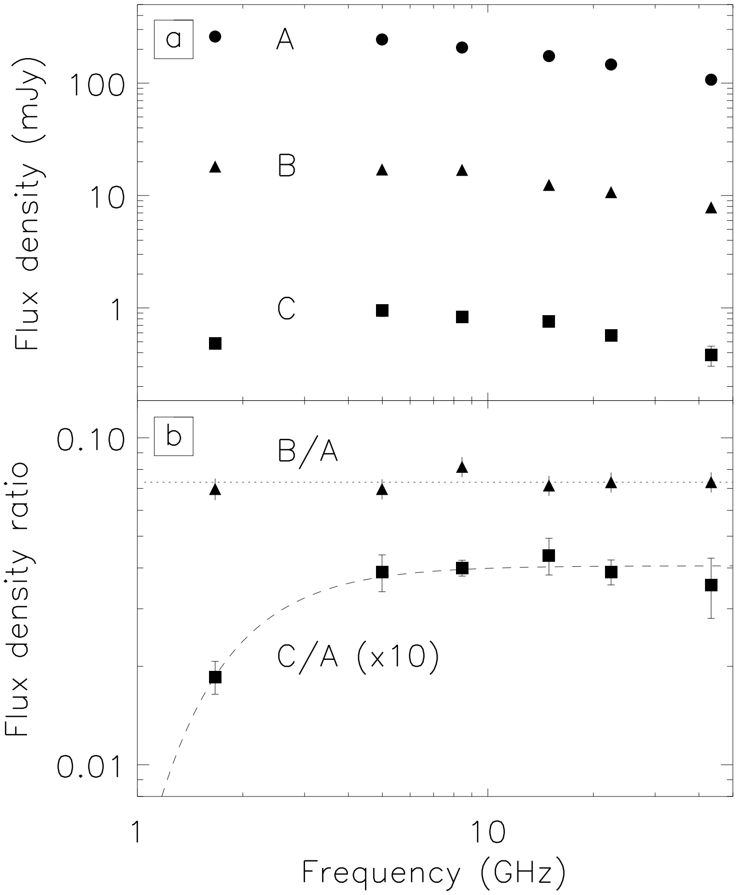

Figure 2. The central radio component and the bright quasar images have similar radio spectra. (a) The flux density of each component as a function of frequency. (b) The flux density ratios relative to A. Results for C/A were multiplied by 10 for display purposes. All the observations at a given frequency from Table 1 and Ref. 15 were combined by averaging the flux density ratios and adopting the total flux density of the most recent measurement, to avoid problems due to source variability and inconsistencies in absolute flux density scale. The only discrepancy between C and A is at 1.7 GHz, where C is fainter than expected for a lensed image. One plausible explanation is free-free absorption due to ionized material $\lesssim$200 parsecs from the lens galaxy nucleus, the approximate position of C. The dashed line is a 2-parameter fit to the function $\mu_{\rm CA} e^{-\tau_\nu}$, using a standard approximation[25] for free-free opacity, $\tau_\nu = 0.08235\, T^{-1.35} \nu^{-2.1} E$, where ν is the frequency (in GHz) and T and E are the temperature (in Kelvins) and emission measure (the integral of n_e^2 over the path length s, in cm^{-6}pc) of the ionized medium. The required opacity $\tau_\nu = 0.7$ at the lens-frame frequency $\nu \approx 3.4$ GHz could be produced by circumnuclear material with, for example, $T = 6000$ and $E = 10^7$ ($n_e = 10^3$ cm^{-3}, $s = 10$ pc), which seems physically reasonable. For comparison, the emission measure is larger than in most individual Galactic H II regions ($E{\sim}10^{5-6}$; e.g., ref. 25), comparable to some ionized clouds around Sgr A ($E{\sim}10^{6-7}$; e.g., ref. 26), and smaller than observed around the nuclei of some radio galaxies ($E{\sim}10^8$, e.g., refs. 27,28). The free-free absorption hypothesis and the nature of the absorbing medium could be tested further with future low-frequency observations.